Desalination and Water Treatment
www.deswater.com
doi: 10.5004/dwt.2023.29723

302 (2023) 129–137
August

Study of graphdiyne biomimetic nanomaterials as fluorescent sensors of ciprofloxacin hydrochloride in water environment

Peilong Xu[a,b], Xuehua Liu[b], Yuling Zhao[b], Dan Lan[a,c], Incheol Shin[a,*]

[a]*Department of Artificial Intelligence Convergence, Pukyong National University, 45 Yongso-ro, Nam-gu, Busan 48513, Republic of Korea, emails: icshin@pknu.ac.kr (I. Shin), 202356105@pukyong.ac.kr (P. Xu), 202256827@pukyong.ac.kr (D. Lan)*
[b]*State Key Laboratory of Bio-Fibers and Eco Textiles, Qingdao University, Shandong, Qingdao 266071, China, emails: liuxuehua@qdu.edu.cn (X. Liu), zhaoyuling@qdu.edu.cn (Y. Zhao)*
[c]*College of Automotive and Information Engineering, Guangxi Eco-engineering Vocational and Technical College, Liuzhou 545004, Guangxi, China*

Received 20 November 2022; Accepted 24 June 2023

ABSTRACT

Ciprofloxacin hydrochloride is widely used in aquaculture industry, and is often used as fishery medicine to prevent and treat bacterial infection diseases in aquatic animals. However, the drug will enter the environment in the form of primitive form or metabolites, directly threatening public health safety and polluting the ecological environment. In this study, based on graphdiyne quantum dot (GDYQDs), a new nanocomplex dopamine-graphdiyne quantum dot (DA-GDYQDs) was prepared using the mussel bionic nanotechnology. And DA-GDYQDs was used to build a fluorescence sensing system for quantitative detection of ciprofloxacin hydrochloride. The experimental results proved that DA-GDYQDs can be used in detecting ciprofloxacin residue in water quickly and effectively.

Keywords: Graphdiyne; Graphdiyne quantum dot; Fluorescence sensor; Bionic nanotechnology

1. Introduction

Ciprofloxacin hydrochloride is the third generation of quinolone. Its molecular formula is $C_{17}H_{18}FN_3O_3{\cdot}HCl{\cdot}H_2O$, molecular weight of 385.82. It is the fluoroquinolone drugs strong antibacterial activity, which can directly act on the bacterial nucleus, inhibit bacterial DNA gyrase, cause its rapid death, and is widely used in fishery production to prevention and control aquatic animal infectious diseases. Studies have shown that ciprofloxacin hydrochloride has more serious liver and kidney toxicity, more intakes will cause human visceral damage, digestive system bleeding, liver and kidney function abnormalities and failure, leukopenia and other diseases, nervous system diseases and allergies can also occur [1]. These drugs applied to water bodies not only act on target organisms to control diseases, but also affect and poison non-target organisms, leading to the imbalance of water micro-ecology and the destruction of ecosystem structure and function [2]. At present, there are many common methods to detect ciprofloxacin hydrochloride, mainly including high performance liquid chromatography, electrochemical analysis, liquid-mass combination analysis, microbial detection and fluorescence analysis [3]. With the emphasis of the environment and health, it is important to develop a highly selective and more sensitive fluorescent probe for the detection of this drug in the water environment [4,5].

Carbon plays a vital role in maintaining life on Earth. Carbon is an interesting atom with three different hybridized states, including sp, sp^2, and sp^3. According to the binding modes of carbon atoms in different hybrid states, various carbon all forms, such as diamond (sp^3), fullerene (sp^2),

* Corresponding author.

carbon nanotubes (CNT, sp^2) and graphene (sp^2) in different hybrid states, have been prepared and successfully used in energy-related fields. The sp hybrid carbon triple bond structure has high conjugation and linear structure and has no cis–trans isomers [6–8]. So, scientists have been eager to prepare carbon all forms containing sp hybrid carbon atoms, which will be key materials for the next generation of energy devices. Baughman et al. [9] predicted a new two-dimensional carbon heterogeneous body (GYs) with alkynyl (sp-C) bridge-connected benzene ring (sp^2-C) structure. According to the number of acetylene units between two adjacent aromatic rings, GYs can be divided into graphdiyne (GY), graphite dinylene (GDY), graphite trinylene (GTY), etc. Due to the high formation energy and flexibility of sp bonds, the study of graphdiyne has been in the theoretical stage. Yuliang Li et al. [10] successfully prepared a large area of graphite inylene film (defined as-graphite inylene, GDY) through *in-situ* Glaser coupling reaction of hexaacetylene benzene (HEB) monomer on copper (Cu). The GDY films show excellent electron conductivity (2.5610^{-1} $S{\cdot}m^{-1}$, comparable to silicon) and high charge carrier mobility (2,105 $cm^2{\cdot}V^{-1}{\cdot}S^{-1}$). Since this major breakthrough, GDY has attracted great attention from scientists about its basic research and practical applications [11]. Many synthesis strategies have been developed, such as autocatalytic growth, template synthesis, chemical vapor deposition, and explosion methods, and have obtained a variety of different morphologies from 1-D nanowires/nanotubes, 2-D nanosheets/nanoparticles to 3-D ordered nanostructure arrays. Due to its excellent performance, GDY is widely used in catalysis, energy storage, solar cells, photovoltaic devices, biological applications, environmental applications and other fields.

Construction of fluorescent polymers based on mussel biomimetic technology is a new method developed in 2015 [12]. The fluorescent polymers prepared by mussel bionic chemistry have both the properties of mussel bionic chemistry and polymer. At present, mussel biomimetic technology is used the study of the structure of fluorescent polymers, which is mainly based on the action of phthalates and polyamines [13]. Materials synthesized by mussel bionic technology are widely used to detect substances, biological probes, and are used for drug-carrying and targeted therapies.

In recent years, mussel bionic technology has been applied to the military, industrial manufacturing industry, medical care, construction industry and other popular industries and fields [14–16]. Mussel bionic technology has become a hot topic among experts and scholars at home and abroad. In nature, the organisms developed through inheritance and survival of the fittest are very different. The synthetic special materials and their "magical" properties and functions make people marvel at the uncanny work of nature. The key and difficulties of nanobiomimetic materials are reflected in the imitation of these natural microscopic substances and structures [17].

In this paper, a new DA-GDYQDs fluorescence sensing system based on mussel bionic was constructed to detect ciprofloxacin hydrochloride residue in water bodies. The results show that DA-GDYQDs demonstrated high sensitivity as well as good selectivity in actual sample detection.

2. Materials and methods

2.1. Preparation of DA-GDYQDs

As a new nanomaterial, graphdiyne quantum dot (GDYQDs), has many excellent fluorescent characteristics compared with traditional organic fluorescent dyes, and has a very broad application prospect in the fields of bioanalytical chemistry, fluorescence immunology, genomics, proteomics and cell biology. In recent years, the application of GDYQDs based on chemical methods has become increasingly prominent, expecting promising fluorescence luminescence performance. As a nanoscale derivative in graphdiyne materials, GDYQDs has both photoluminescence and graphdiyne characteristics. Advantages of GDYQDs include excellent photostability, adjustable photic luminescence, better solubility, chemical inertia, high biocompatibility and easy functionalization. Meanwhile, GDYQDs has wide applications in fields such as optical biosensing and biological imaging.

Marine mussel (Mytilus) is a double shell mollusk, and mainly living in the coastal coast. It is one of the common organisms along the coast, belongs to the mussel family (Mytilidae). Marine mussels have corrosion resistance, acid and alkali resistance, oxidation resistance and heat resistance. Mussel bionic technology is used in many fields, and the surface modification of the material in the actual operation process is greatly limited, mainly due to the complex experimental operation process and reaction conditions and special requirements for the material. Therefore, the most important thing is to develop simple and effective methods as well as simple reaction conditions. Mussel bionic functionalized material technology has made up for the lack of existing technical means, and made great contributions to the application of the surface adhesion properties of many materials, making it gradually become a hot topic in many interdisciplinary fields such as bionic materials, such as bionics, chemistry, and biological medicine, etc. The rapid development of mussel bionics technology with nanoscience provides a variety of nanomaterials with highly controlled and unique optical, electronic, magnetism and catalytic properties. Different nanomaterials play very different roles in different sensing systems, including their fixation for biomolecules, catalyzing electrochemical reactions, improving the electron transfer between biomolecules and electrodes, labeling biomolecules, and acting as reactive substances.

Inspired by the adhesion proteins of marine mussels, Waite et al. [18] first analyzed the composition of the adhesion proteins, which showed that the amino acid structure fragment was composed of dopa (DOPA) residue structure, hydroxyproline residue structure and lysine residue structure, and the higher the DOPA concentration, the stronger the adhesion effect. Murphy et al. [19] speculated that dopamine and its dopamine-like derivatives also have a strong adhesion to adsorbing most of the surface layer of the materials. Further research on the dopamine polymerization mechanism shows that in aqueous solution, the phenolic hydroxyl pole of dopamine is easy to generate dopamine quinone compounds with catechol structure, mainly due to oxidation (or other oxidative conditions). The process of dopamine self-oxidation is relatively flat, and the principle of dopamine oxidation automerization of polydopamine is mainly through the dopamine and dopamine quinone ambiguity reaction, producing

free radicals and even synthetic cross-linking bonds, while generating cross-linked composite polydopamine coating, and adsorbed on the surface of the matrix material.

In this study, DA-GDYQDs is synthesized based on mussel bionic nanotechnology. Transmission electron microscopy (TEM), infrared spectroscopy, UV spectroscopy, and fluorescence spectroscopy were characterized, and the microscopic particle structure of DA-GDYQDs was observed. Its stability was also tested by light time, different concentrations of NaCl solution, and different pH.

2.1.1. Reagents and instruments

The main reagents used in the experiment were provided by Macklin Inc. Macklin is founded in 2013 and located in Shanghai Pudong. The specific types of reagents are shown in Table 1.

Table 1
Main reagents for the experiments

Reagents	Specifications	Manufacturers
Graphdiyne powder	Powder, diameter: 40–100 nm, thickness: 3–4 nm	Macklin Inc.
NaOH	Spectroscopically pure	Macklin Inc.
Citric acid	Spectroscopically pure	Macklin Inc.
Isopropanol	Spectroscopically pure	Macklin Inc.
Dopamine	Spectroscopically pure	Macklin Inc.
Alcohol	Spectroscopically pure	Macklin Inc.

2.1.1.1. Experimental reagents

The main instruments used in the experiment are shown in Table 2. The manufacturers involved include Mettler Toledo located in Zurich, Switzerland; Leici Shanghai, located in Pudong, Shanghai, China; Shumei located in Kunshan, Shanghai, China; Ketai Zhengzhou, located in Zhengzhou, Henan, China; ZEISS located in Oberkohen, Badenburg, Germany; Persee located in Beijing, China; Thermo Fisher Scientific, located in Massachusetts, USA; Varian, located in Palo Alto, California, USA.

2.1.1.2. Laboratory instruments

Table 2
Main experimental instruments and equipment's

Instruments	Types	Manufacturers
Electronic balance	XPR105	Mettler Toledo
Acidometer	PHS-3C	Leici Shanghai
Ultrasonic cleaner	KQ-100DE	Shumei
Reaction kettle	GK-100	Ketai Zhengzhou
Field-emission scanning electron microscope	Sigma 300	ZEISS
Ultraviolet spectrophotometer	TU1900	Persee
Fourier-transform infrared spectrometer	iS50	Thermo Fisher Scientific
Fluorospectrophotometer	Eclipse	Varian

2.1.2. Preparation of graphdiyne quantum dot

2.1.2.1. Treatment of the GDY powder

After the copper plates were washed with hydrochloric acid (4 mol·L^{-1}), they were washed again with water and ethanol under ultrasound waves. Copper plates and pyridine (60 mL) were placed in a three-well flask and heated for 1 h at 120°C under nitrogen protection. In an ice bath, hexaacetylene benzene (200 mg) was dissolved in 50 mL tetrahydrofuran (THF) and nitrogen was purged for 30 min. 2.5 mL tetrahydrofuran was added to 1 mol·L^{-1} tetra-n-butylammonium Fluoride (TBAF) and stirred at low temperature in nitrogen for 15 min. The reaction mixture was diluted with ethyl acetate, washed three times with saturated sodium chloride, then dried and filtered. The dried hexaacetylbenzene precursor was dissolved in 50 mL pyridine, transferred to a nitrogen-protected constant addition funnel, and dropped into a mixture containing pyridine (60 mL) and copper sheets at 80°C for 10 h. After the addition of the deprotective compound, the mixture was maintained at 120°C for 3 d. After the reaction, the pyridine was evaporated by freeze-drying. The products were collected by centrifugation, then washed continuously with dimethylformamide (80°C) and ethanol (70°C), and dried to obtain the GDY powder.

2.1.2.2. Preparation of GDYQDs

GDY powder (10 mg) was mixed with concentrated sulfuric acid (98%, 2.5 mL) and hydrogen peroxide (30%, 1.0 mL), and the mixture was stirred in ice water for 1 h. The product was centrifuged (8,000 rpm, 10 min) and washed with ultrapure water, GDY water suspension (10 mL, 0.5 mg·mL^{-1}) was prepared by ultrasonic (120 W, 30 kHz) for 24 h. The resulting solution was heated in an oil bath (100°C, 6 h), and the supernatant was obtained by centrifugation to get GDYQDs.

2.1.2.3. Preparation of DA-GDYQDs

GDYQDs was added into 20 mL isopropanol, and centrifuged at 10,000 rpm to get the oily liquid, a small amount of water was added to disperse the liquid, and then isopropanol was added in again. This process was repeated more than three times to obtain pure intermediates. Add 100 μL of the above solution into 10 mL of water, stir well, add 20 mg of dopamine (DA), and then appropriate tris solution (pH = 8.5) for quick stirring and dispersing until the mixed solution is pH = 8.5. Around 3 min, the solution color changed from transparent pale yellow to light gray, indicating self-aggregation of DA. After stirring for 10 h at room temperature, a grey-black suspension was obtained. It was centrifuged at 10,000 rpm to remove large particles and yield DA-GDYQDs.

2.1.3. TEM characterization

Turn on the total power supply of TEM, the cooling water, and the vacuum switch in turn, and the vacuum system will automatically vacuum. Generally, after 15~20 min, after the high vacuum indicator light is on, the transmission

electron microscope start to work. Connect the power supply in the transmission electron mirror cylinder, supply power to the electron gun and lens, and add high pressure to the electron gun from low speed to high speed until the required value.

2.1.4. Fourier-transform infrared spectroscopy characterization

Use OMNIC software, click detection button, turn the screen to the measurement interface, initialize the instrument, prepare potassium bromide blank and sample tablet. Put the pressed potassium bromide blank sheet into the sample frame in the sample bin of the spectrograph; click the background under the measurement button to confirm the acquisition of the background spectrum. After the collection, put the sample into the spectrometer, and close the warehouse cover for measurement.

2.2. DA-GDYQDs nanocomposites detect ciprofloxacin hydrochloride in water drug residues

In recent years, the existing materials has been unable to fully meet people's production and living needs in the field of materials. Therefore, the improvement of nanomaterials is mainly reflected in the regulation of material surface performance and the focus on the surface modification research of materials, for example, improving the performance of materials and extending the service life. There are many surface modification methods for materials, including surface coating, chemical modification, self-assembly monolayer, surface grafting, layer by layer self-assembly, etc. The methods can modify the material surface to increase acid and alkali resistance, enhance its corrosion resistance, oxidation resistance and heat resistance. The traditional method of the surface modification of the material is mainly limited by the specific requirements of the material or shape and the complex reaction conditions. Therefore, it is urgent to develop a simple and effective material surface modification method. With the emergence of mussel bionic technology to solve the shortcomings of traditional methods, it has gradually become the research hotspot of many interdisciplinary disciplines, such as materials science, bionics, bionics, chemistry, biomedicine, etc.

Ciprofloxacin hydrochloride is a common synthetic quinolone antibiotic with the advantages of low toxicity and good absorption effect, so it is widely used in the disease treatment of livestock and poultry animals. However, this medicine can easily accumulate in animals and enter the human body through the food chain, forming a resistance to drugs and affecting the relevant clinical efficacy. Therefore, the EU and United Nations Food and Agriculture organizations have set maximum residue limits for quinolones. In addition, announcements No. 235 and No. 2292 issued by the Ministry of Agriculture also made clear provisions on the scope and amount of quinolone drugs such as ciprofloxacin hydrochloride. Therefore, it is important to develop a convenient and reliable assay for detecting quinolone residues in animal foods. At present, the detection methods of quinolone residues in animal foods mainly include high-performance liquid chromatography (HPLC) and HPLC tandem mass spectrometry, but the complex matrix interference limited the application of liquid chromatography, and the current detection methods have problems such as complex pretreatment, time consuming and low recovery. Therefore, a simple fluorescence measurement was developed to detect quinolones in fish meat based on graphdiyne quantum dots. Due to its simplicity, convenience and high sensitivity, it has great potential in future practical applications.

2.2.1. Reagents and instruments

The main reagents used in the experiment are shown in Table 3, with Solarbio Life Science located in Zhongguancun Science and Technology Park, Tongzhou District, Beijing, China; Alfa Aesar is located in Fengxian District, Shanghai, China; Sigma-Aldrich is located in Fort Miami, Ohio, USA. The main instruments used in the experiment are shown in Table 4, with IKA located in Staufenim Breisgau, Germany; Varian, located in Palo Alto, California, USA; Mettler Toledo located in Zurich, Switzerland; Leici Shanghai, located in Pudong, Shanghai, China; Shumei located in Kunshan, Shanghai, China; Persee located in Beijing, China.

All chemicals were spectroscopic pure and were not further purified prior to use. The resistivity of the experimental water was higher than 18 MΩ·cm^{-1}.

Table 4
Instruments for experiments

Instrument names	Types	Manufacturers
Fluorospectrophotometer	Eclipse	Varian
Heated magnetic stirrer	RW20	IKA
Electronic balance	XPR105	Mettler Toledo
Acidometer	PHS-3C	Leici Shanghai
Ultrasonic cleaner	KQ-100DE	Shumei
Ultraviolet spectrophotometer	TU1900	Persee

Table 3
Main reagents used for the experiments

Reagents	Specifications	Manufacturers
Ciprofloxacin hydrochloride	Spectroscopically pure	Solarbio Life Science
N,N-Dimethylacetamide	Spectroscopically pure	Alfa Aesar
Monometallic sodium orthophosphate	Spectroscopically pure	Sigma-Aldrich
1-(3-ditrimethylinepropyl)-3-ethylcarbondiamine hydrochloride	Spectroscopically pure	Sigma-Aldrich

2.2.2. Fluorescence detection of ciprofloxacin hydrochloride

200 μg·L^{-1} DA-GDYQDs was added to 5 μg·L^{-1} ciprofloxacin hydrochloride solution, phosphate buffered saline (PBS) solution with pH = 5, 6, 7, 8, 9, and pH = 10 was added to 1.5 mL, respectively. The solutions were shaken for 20 min at room temperature, and the above operation was repeated twice. Place the 6 sets of solutions for detection. Light excitation was excited at 400 nm and the fluorescence emission spectrums of the solutions were recorded. The effects of these interfering substances on the test results were detected using coexisting substances including glycine (Gly), sulfadimidine, glucose, vitamin C and bovine serum albumin (BSA).

3. Results

3.1. Characterization of the DA-GDYQDs

3.1.1. Characterization of TEM

As shown in Fig. 1, the microscopic morphology and particle size distribution of GDYQDs (A) and DA-GDYQDs (b) were observed by TEM characterization. It can be seen that the GDYQDs are spherical, neatly distributed, and uniform in size, with good dispersion, and no aggregation between the particles. Fig. 1a is the particle size distribution map of GDYQDs, with an average radius of about 2.5 nm. As shown in Fig. 1b, DA-GDYQDs have approximate spherical structures with large size distribution, good single dispersion, irregular particles, and no aggregation between each other. The average diameter of DA-GDYQDs is about 60 nm, with a large particle-size distribution.

3.1.2. Characterization of Fourier-transform infrared spectroscopy

Fig. 2 shows the infrared spectral characterizations of DA-GDYQDs (a) and GDYQDs (b). GDYQDs (b) showed phenyl hydroxyl characteristic peak at 3,430 cm^{-1}, amino characteristic peak at 2,428 cm^{-1}, and carbon–carbon double bonds characteristic peak at 1,639 cm^{-1}. DA-GDYQDs (a) shows characteristic absorption peaks at 3,600 and 3,200 cm^{-1}, mainly due to the expansion vibration of O–H and N–H, and the absorption peak at 2,445 cm^{-1} is mainly due to C–H vibration, and the absorption peak at 1,060 cm^{-1} comes from C–O vibration. The absorption peaks are quite different between the two substances, and the peak of DA-GDYQDs has a wide absorption band, mainly due to the absorption of the –COOH group in the GDYQDs. DA-GDYQDs, with an additional epoxy group in the structure, the absorption peak changed at 1,120 cm^{-1}, mainly due to self-polymerization on its surface after the introduction of DA. Fourier-transform infrared spectroscopy characterization of the two substances showed that DA-GDYQDs have been synthesized successfully. In addition, DA-GDYQDs contains phenyl hydroxyl group (3,430 cm^{-1}), group (1,735 cm^{-1}), carbon–carbon double bond (1,639 cm^{-1}), and methylene group (1,400 cm^{-1}). These functional groups are hydrophilic groups, giving DA-GDYQDs excellent hydrophilicity, quickly soluble in water, and convenient for experimental operation.

3.1.3. Characterization of the UV-Visible spectra

Fig. 3 shows the UV-Visible absorption spectral characterization of DA-GDYQDs. It can be seen from the figure

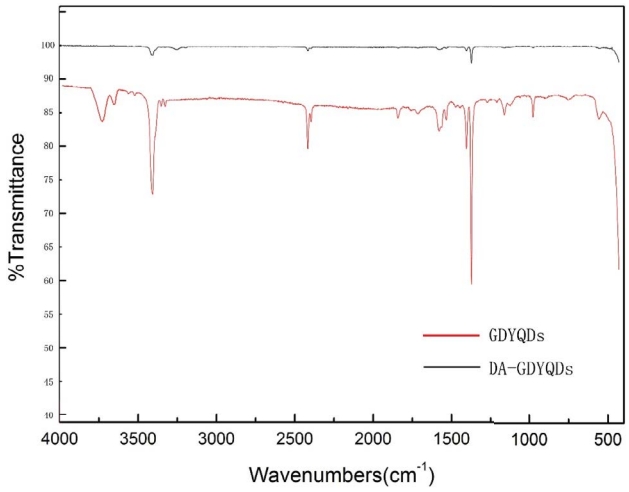

Fig. 2. Fourier-transform infrared spectroscopy images of GDYQDs and DA-GDYQDs.

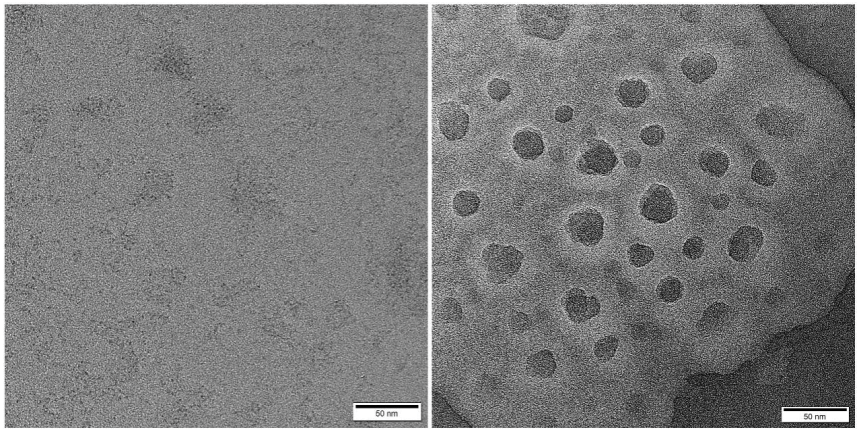

Fig. 1. Transmission electron microscopy images of GDYQDs and DA-GDYQDs.

that, DA-GDYQDs has a major absorption peak at 400 nm mainly from the leap absorption of n-* in GDYQDs, which is similar to the UV absorption spectrum of graphdiyne oxide in the literature. The peak at 400 nm was weaker than that previously reported for GDYQDs, probably due to the introduction of DA.

3.1.4. Characterization of the fluorescence spectra

Fig. 4 shows the fluorescence spectral characterization of DA-GDYQDs. The emission peak was at 476 nm, with high fluorescence intensity, better peak pattern and no dragging. Fig. 5a shows the fluorescence spectrum of GDYQDs at different excitation wavelengths. The spectral characterization agrees with the previously reported GDYQDs, and the position of the fluorescence peaks changes with the excitation wavelength change.

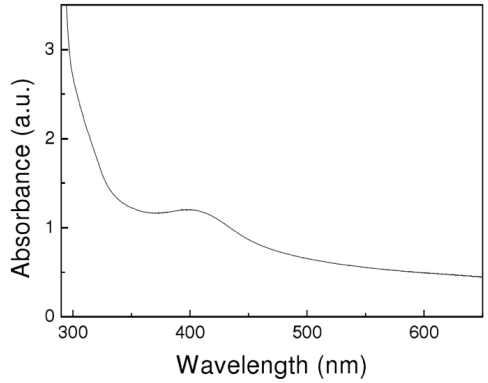

Fig. 3. UV-Visible absorption spectra of the DA-GDYQDs.

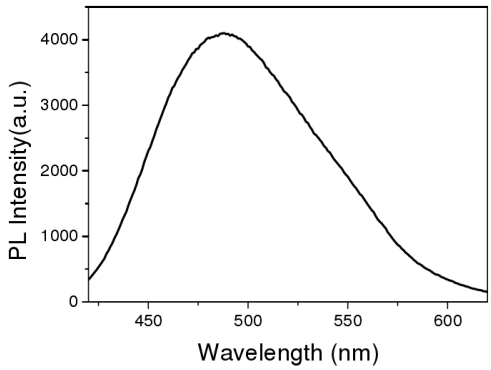

Fig. 4. Fluorescence spectra of the DA-GDYQDs.

3.1.5. Stability research of DA-GDYQDs

Fig. 6 shows the results of various stability studies of DA-GDYQDs. Fig. 6a show the changes in DA-GDYQDs emission intensity as monitored under continuous UV lamp illumination. No significant change in emission intensity at 48 h continuous irradiation, demonstrating very good photostability of DA-GDYQDs. As shown in Fig. 6b, the luminescence did not show significant changes in the 0.08 M NaCl solution, indicating a high tolerance of DA-GDYQDs to the concentration of salt ions.

Finally, the stability of the DA-GDYQDs in different pH-value environments was tested. As shown in Fig. 6c, the fluorescence intensity of pH was largely unaffected between 5 and 7, increasing significantly at a pH of 8 and decreasing significantly between 9 and 10. This is mainly because that in weak alkaline condition, DA-GDYQDs forms a highly conjugated structure with a stronger skeleton, high quantum production rate and strong luminescence [20–22].

3.1.6. Discussion on characterization of DA-GDYQDs

Characterization studies including TEM, infrared spectroscopy, UV-Visible spectroscopy, and fluorescence spectroscopy demonstrate an excellent particle structure of DA-GDYQDs. Experimental results of different light times, different concentrations of NaCl solution and the stability of different pH on DA-GDYQDs show that DA-GDYQDs is basically unaffected by light time, different salinity and different pH, and has good stability [23].

3.2. Other influencing factors

3.2.1. Effects of different pH on the detection system

In Fig. 7, the red column shows that, the highest fluorescence intensity at pH = 8 in the presence of ciprofloxacin

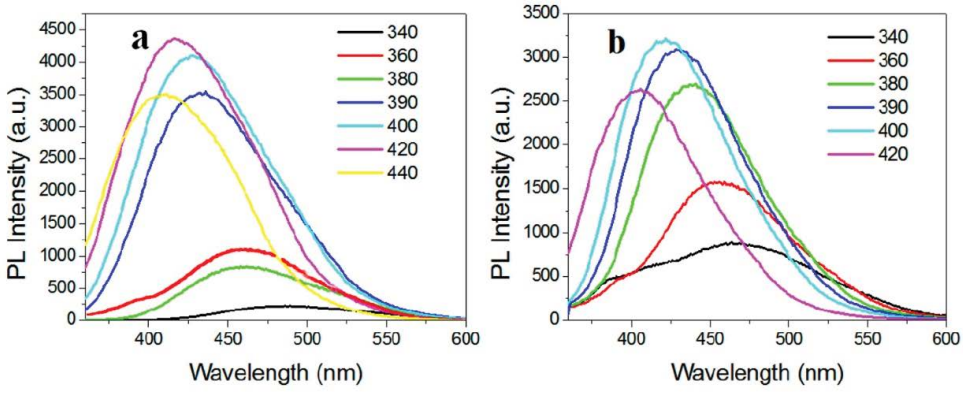

Fig. 5. Fluorescence spectra at different excitation wavelengths: (a) GDYQD and (b) DA-GDYQDs.

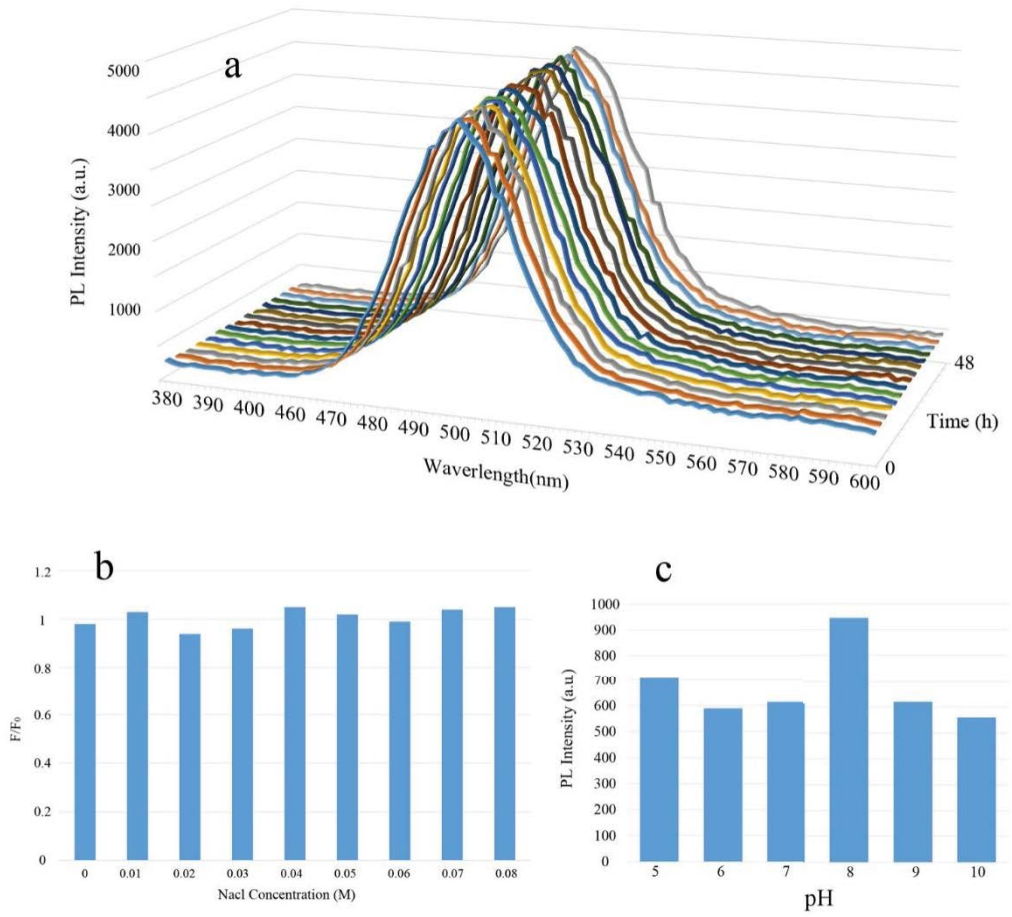

Fig. 6. Stability test results of DA-GDYQDs: (a) photostability, (b) fluorescence effects of different concentrations of NaCl and (c) different pH on DA-GDYQDs.

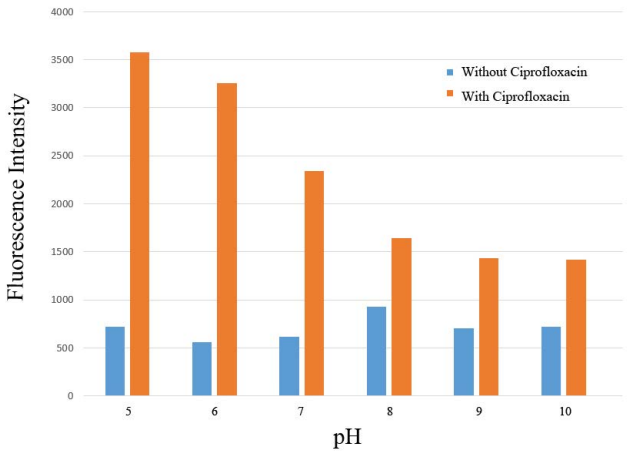

Fig. 7. Effects of different pH on DA-GDYQDs under different ciprofloxacin hydrochloride conditions.

hydrochloride. The green column shows that, in the presence of ciprofloxacin hydrochloride, the fluorescence intensity of DA-GDYQDs gradually decreases with increasing pH values until it recovers slightly at pH = 10. The test results showed that the DA-GDYQDs fluorescence intensity was

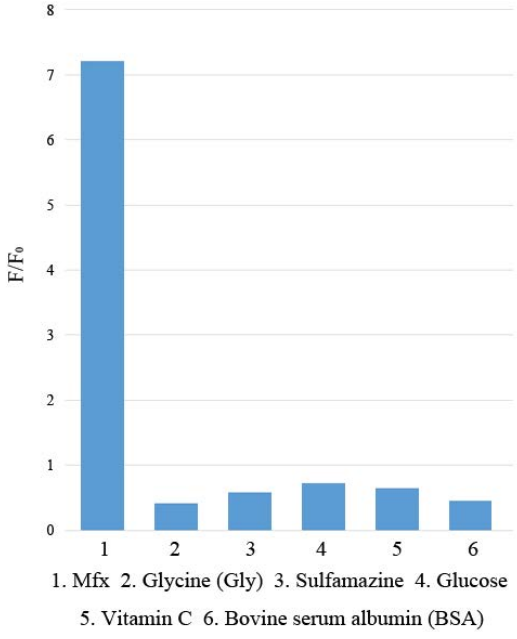

Fig. 8. Interference of fluorescence intensity on ciprofloxacin hydrochloride.

significantly enhanced after adding ciprofloxacin hydrochloride, and was maximum at pH = 5. This is due to the acid effect of DA-GDYQDs in acidic conditions and some hydrolysis of ciprofloxacin hydrochloride in neutral or alkaline conditions, which also affects DA-GDYQDs binding to ciprofloxacin hydrochloride. Therefore, the acidic conditions promoted the reaction of DA-GDYQDs with ciprofloxacin hydrochloride, so the PBS with pH = 5 was chosen as the buffer solution for subsequent experiments.

3.2.2. Interference research

There are usually some other substances present in the experiments that may affect the actual sample detection [24]. Therefore, to assess the accuracy of the proposed method, the effect of different potential interfering substances on the intensity of fluorescence values was examined under the same concentration of ciprofloxacin hydrochloride (4.0×10^{-6} mol·L^{-1}). In Fig. 8, F_0 and F represent the fluorescence intensity in the absence and presence of the interfering material, and F/F_0 represents the ratio of the fluorescence intensity F_0 and F, respectively. The results showed that the tolerable concentrations ratio of glycine (Gly), sulfadimidine, glucose, vitamin C and BSA and 4.0×10^{-6} mol·L^{-1} ciprofloxacin hydrochloride were more than 104 times. It is found that these substances have little effect on the detection of ciprofloxacin hydrochloride, thus proving the high accuracy of this method.

4. Discussion

Characterization studies such as TEM, infrared spectroscopy, UV-Visible spectroscopy, and fluorescence spectroscopy have demonstrated favorable particle structure of DA-GDYQDs. The results of light time, different concentrations of NaCl solution, and the stability of different pH on DA-GDYQDs show that DA-GDYQDs is basically not affected by light time, different salinity and different pH, and has good stability. In the study, ciprofloxacin hydrochloride drug residues in water were detected based on a new method established by DA-GDYQDs as a fluorescent sensor. Experimental results show that the proposed method has high sensitivity, good selectivity and low detection limit, and good linear relationship.

5. Conclusion

In this study, a new method to detect the drug content of ciprofloxacin hydrochloride in water using DA-GDYQDs as a fluorescence probe. The experimental results show that the fluorescent probe has high sensitivity and better selectivity. The correlation of quinolone drug concentration with the fluorescence intensity ratio F/F_0 under the optimal experimental conditions provided the basis for quantitative analysis, with ciprofloxacin hydrochloride being linearly ranging from 4×10^{-8} to 2×10^{-6} mol·L^{-1} and a detection limit of 2.16×10^{-8} mol·L^{-1}. This method can be used for quantitative detection of quinolones in water and with satisfactory results.

Acknowledgment

This work was supported by the Ministry of Education of the Republic of Korea and the National Research Foundation of Korea (NRF-NRF-2020R1F1A1076316).

References

[1] X.-Y. Zhang, Y.-S. Yang, W. Wang, Q.-C. Jiao, H.-L. Zhu, Fluorescent sensors for the detection of hydrazine in environmental and biological systems: recent advances and future prospects, Coord. Chem. Rev., 417 (2020) 213367, doi: 10.1016/j.ccr.2020.213367.
[2] Y. Wu, X. Liu, Q. Wu, J. Yi, G. Zhang, Differentiation and determination of metal ions using fluorescent sensor array based on carbon nanodots, Sens. Actuators, B, 246 (2017) 680–685.
[3] J. He, P. Xu, R. Zhou, H. Li, H. Zu, J. Zhang, Y. Qin, X. Liu, F. Wang, Combustion synthesized electrospun InZnO nanowires for ultraviolet photodetectors, Adv. Electron. Mater., 4 (2022) 2100997, doi: 10.1002/aelm.202100997.
[4] J. Chen, A. Zheng, A. Chen, Y. Gao, C. He, X. Kai, G. Wu, Y. Chen, A functionalized gold nanoparticles and Rhodamine 6G based fluorescent sensor for high sensitive and selective detection of mercury(II) in environmental water samples, Anal. Chim. Acta, 599 (2007) 134–142.
[5] F. Wang, Z. Gu, W. Lei, W. Wang, X. Xia, Q. Hao, Graphene quantum dots as a fluorescent sensing platform for highly efficient detection of copper(II) ions, Sens. Actuators, B, 190 (2014) 516–522.
[6] P. Xu, J. Cao, C. Yin, L. Wang, L. Wu, Quantum chemical study on the adsorption of megazol drug on the pristine BC_3 nanosheet, Supramol. Chem., 33 (2021) 63–69.
[7] H. Wu, C. Tong, A specific turn-on fluorescent sensing for ultrasensitive and selective detection of phosphate in environmental samples based on antenna effect-improved FRET by surfactant, ACS Sens., 3 (2018) 1539–1545.
[8] H. Li, P. Xu, D. Liu, J. He, H. Zu, J. Song, J. Zhang, F. Tian, M. Yun, F. Wang, Low-voltage and fast-response SnO_2 nanotubes/perovskite heterostructure photodetector, Nanotechnology, 32 (2021) 375202, doi: 10.1088/1361-6528/ac05e7.
[9] S.L. Hsu, A.J. Signorelli, G.P. Pez, R.H. Baughman, Highly conducting iodine derivatives of polyacetylene: Raman, XPS and X-ray diffraction studies, J. Chem. Phys., 69 (1978) 106–111.
[10] G. Li, Y. Li, H. Liu, Y. Guo, Y. Li, D. Zhu, Architecture of graphdiyne nanoscale films, Chem. Commun., 46 (2010) 3256–3258.
[11] P. Xu, N. Na, S. Gao, C. Geng, Determination of sodium alginate in algae by near-infrared spectroscopy, Desal. Water Treat., 168 (2019) 117–122.
[12] F. Du, L. Sun, Q. Zen, W. Tan, Z. Cheng, G. Ruan, J. Li, A highly sensitive and selective "on-off-on" fluorescent sensor based on nitrogen doped graphene quantum dots for the detection of Hg^{2+} and paraquat, Sens. Actuators, B, 288 (2019) 96–103.
[13] P. Xu, N. Na, Study on antibacterial properties of cellulose acetate seawater desalination reverse-osmosis membrane with graphene oxide, J. Coastal Res., 105 (2020) 246–251.
[14] H. Liu, J. Ding, K. Zhang, L. Ding, Construction of biomass carbon dots based fluorescence sensors and their applications in chemical and biological analysis, TrAC, Trends Anal. Chem., 118 (2019) 315–337.
[15] P. Xu, L. Cui, S. Gao, N. Na, A.G. Ebadi, A theoretical study on sensing properties of in-doped ZnO nanosheet toward acetylene, Mol. Phys., 120 (2022) e2002957, doi: 10.1080/00268976.2021.2002957.
[16] Y. Cheng, H. Zhang, B. Yang, J. Wu, Y. Wang, B. Ding, J. Huoa, Y. Li, Highly efficient fluorescence sensing of phosphate by dual-emissive lanthanide MOFs. Dalton Trans., 47 (2018) 12273–12283.

[17] Q. Yang, J. Li, X. Wang, H. Peng, H. Xiong, L. Chen, Strategies of molecular imprinting-based fluorescence sensors for chemical and biological analysis, Biosens. Bioelectron., 112 (2018) 54–71.
[18] V.V. Papov, T.V. Diamond, K. Biemann, J.H. Waite, Hydroxyarginine-containing polyphenolic proteins in the adhesive plaques of the marine mussel Mytilus edulis, J. Biol. Chem., 270 (1995) 20183–20192.
[19] W.L. Murphy, K.O. Mercurius, S. Koide, M. Mrksich, Substrates for cell adhesion prepared via active site-directed immobilization of a protein domain, Langmuir, 20 (2004) 1026–1030.
[20] Y. Xian, K. Li, Hydrothermal synthesis of high-yield red fluorescent carbon dots with ultra-narrow emission by controlled O/N elements, Adv. Mater., 34 (2022) 2201031, doi: 10.1002/adma.202201031.
[21] S. Reagen, Y. Wu, X. Liu, R. Shahni, J. Bogenschuetz, X. Wu, Q.R. Chu, N. Oncel, J. Zhang, X. Hou, C. Combs, A. Vasquez, J.X. Zhao, Synthesis of highly near-infrared fluorescent graphene quantum dots using biomass-derived materials for *in vitro* cell imaging and metal ion detection, ACS Appl. Mater. Interfaces, 13 (2021) 43952–43962.
[22] X. Wang, J. Yu, W. Ji, M. Arabi, L. Fu, B. Li, L. Chen, On–off–on fluorescent chemosensors based on N/P-codoped carbon dots for detection of microcystin-LR, ACS Appl. Nano Mater., 4 (2021) 6852–6860.
[23] H. Wang, L. Da, L. Yang, S. Chu, F. Yang, S. Yu, C. Jiang, Colorimetric fluorescent paper strip with smartphone platform for quantitative detection of cadmium ions in real samples, J. Hazard. Mater., 392 (2020) 122506, doi: 10.1016/j.jhazmat.2020.122506.
[24] X. Wang, J. Yu, X. Wu, J. Fu, Q. Kang, D. Shen, J. Li, L. Chen, A molecular imprinting-based turn-on ratiometric fluorescence sensor for highly selective and sensitive detection of 2,4-dichlorophenoxyacetic acid (2,4-D), Biosens. Bioelectron., 81 (2016) 438–444.